

Supporting Information for: Novel Ternary Transition Metal Oxide Solid solution: Mesoporous Ni-Mn-Co-O Nanowire Arrays as Integrated Anode for High-Power Lithium-ion battery

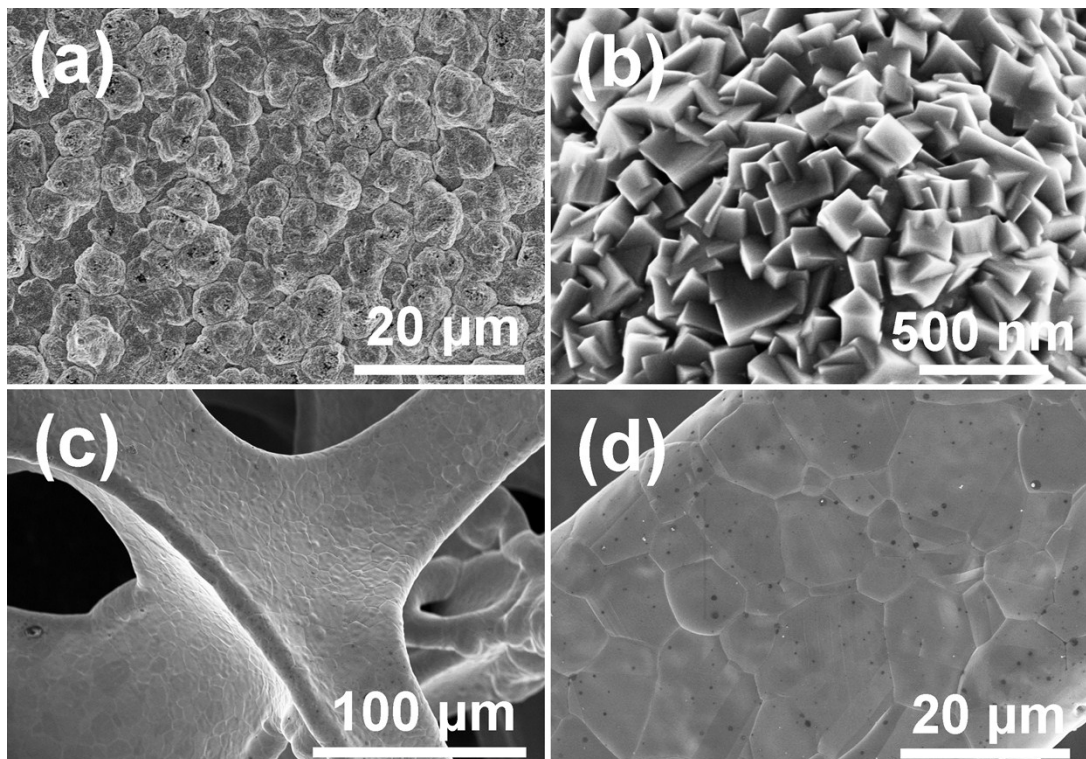


Fig.S1 (a) Low and (b) high magnification SEM images of Cu foil, and (c) Low and (d) high magnification SEM images of the 3D network structure of Cu foam.

* In order to improve the adhesion between Cu foil substrate and NMCO nanowires, the Cu foil is annealed at 400 °C for 2 h in Ar atmosphere before hydrothermal, which makes the surface of Cu foil generate an abundant nanostructure plane. The nanostructure plane can provide abundant active sites for nanowire attachment.

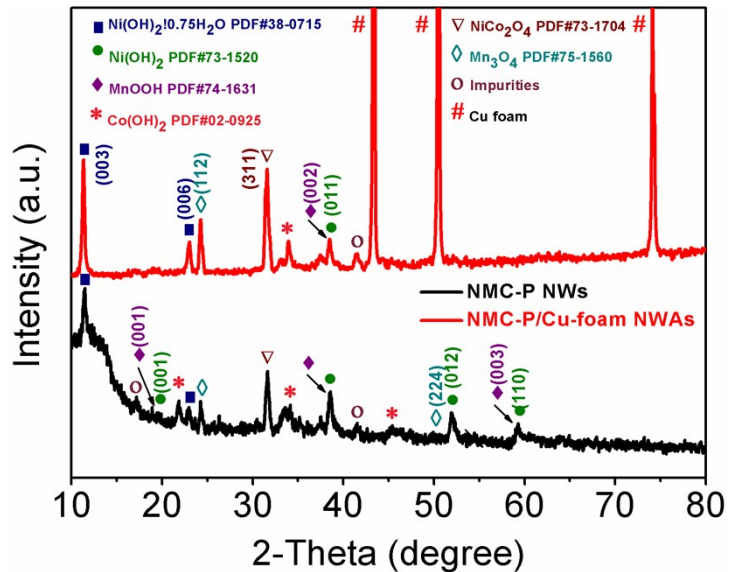


Fig.S2 XRD patterns for two precursors of NMC-P and NMC-P/Cu-foam NWAs.

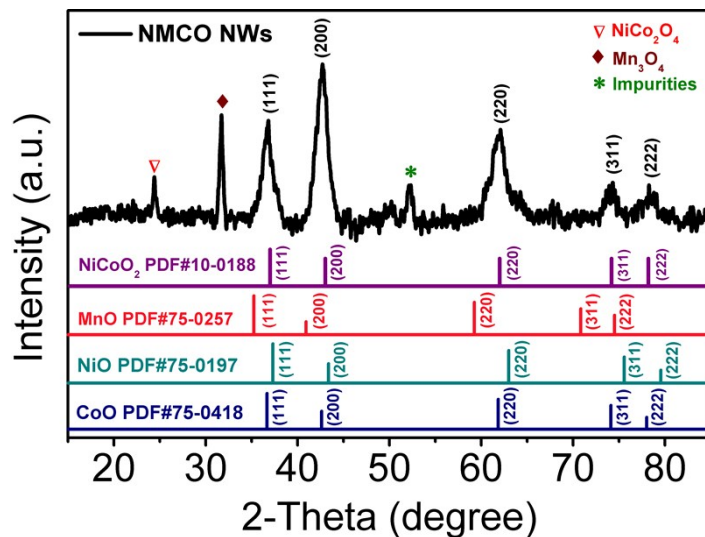


Fig.S3 XRD patterns of the NMCO NWs sample.

Tab.S1 The Crystal parameter for MnO, NiO, CoO, and NiCoO₂.

| Phase | PDF card | Space group | (hkl) | 2-Theta (degree) | | | | D _{hkl} (10 ⁻¹ nm) | | | |
|--------------------------|----------|-------------|-----------|------------------|--------|-------|--------------------|--|-------|-------|--------------------|
| | | | | MnO | NiO | CoO | NiCoO ₂ | MnO | NiO | CoO | NiCoO ₂ |
| MnO | 75-0257 | Fm-3m | (1 1 1) | 35.24 | 37.319 | 36.68 | 36.81 | 2.545 | 2.407 | 2.448 | 2.440 |
| NiO | 75-0197 | Fm-3m | (2 0 0) | 40.91 | 43.362 | 42.61 | 42.82 | 2.204 | 2.085 | 2.120 | 2.110 |
| CoO | 75-0418 | Fm-3m | (2 2 0) | 59.24 | 62.995 | 61.84 | 61.79 | 1.558 | 1.474 | 1.499 | 1.500 |
| NiCoO₂ | 10-0188 | F | (3 1 1) | 70.84 | 75.56 | 74.10 | 73.99 | 1.329 | 1.257 | 1.278 | 1.280 |
| | | | (2 2 2) | 74.51 | 79.57 | 78.00 | 77.99 | 1.273 | 1.204 | 1.224 | 1.224 |

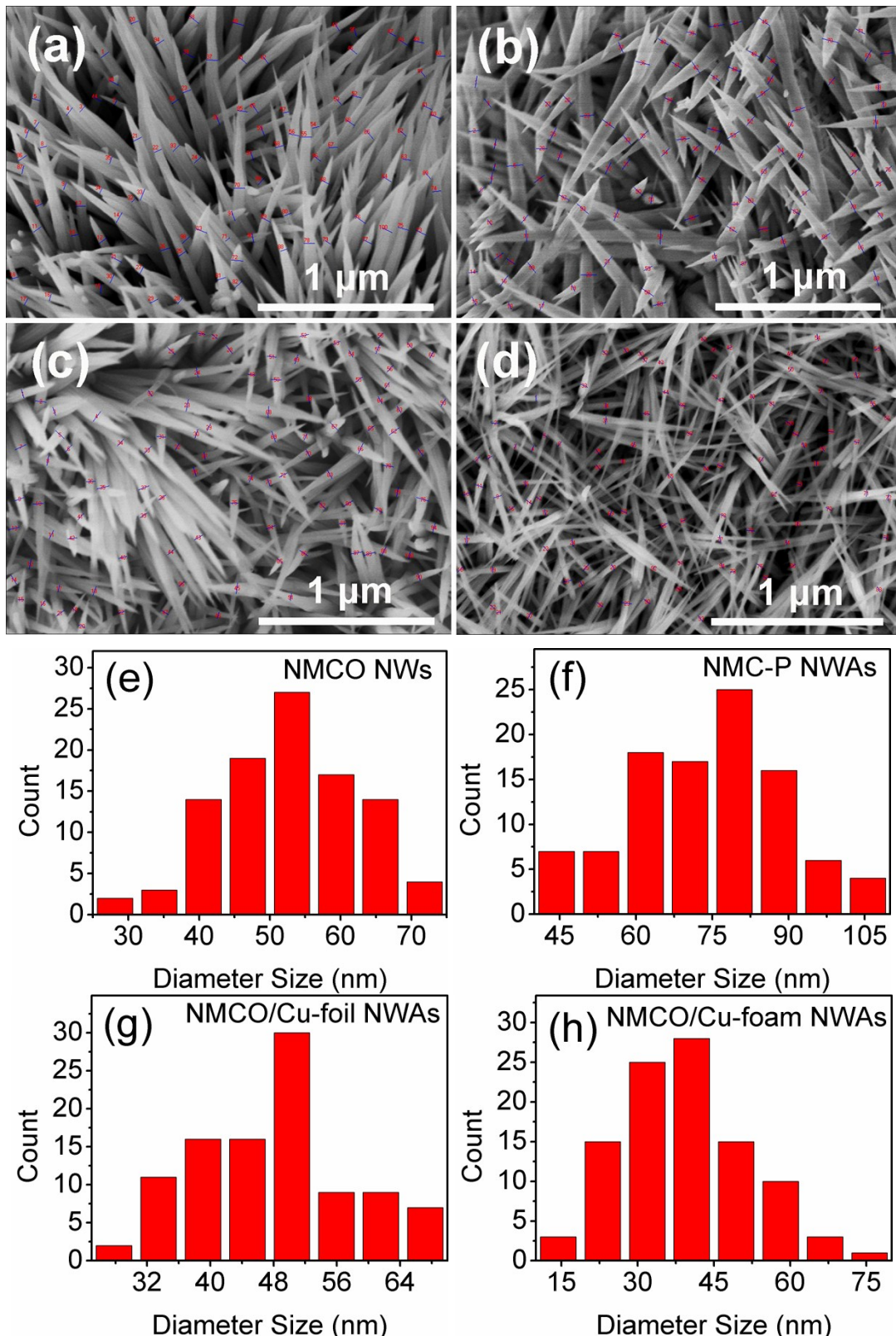
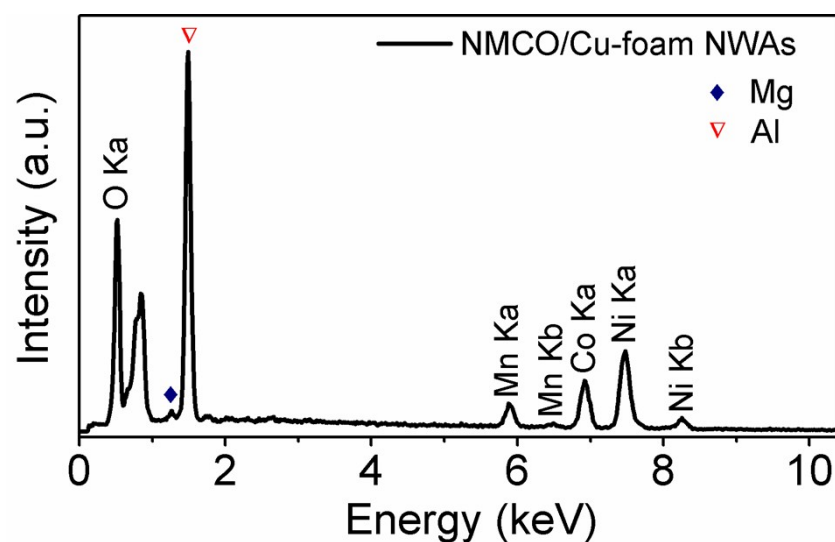


Fig.S4 SEM image sampling and diameter frequency distribution for (a) and (e) NMCO NWs, (b) and (f) NMC-P NWAs, (c) and (g) NMCO/Cu-foil NWAs, and (d) and (h) NMCO/Cu-foam NWAs.

Tab.S2 The average diameter of four samples counted from the SEM image of Fig. S4.

| Sample | Average Diameter (nm) |
|-------------------|-----------------------|
| NMCO NWs | ~53 |
| NMC-P/Cu NWAs | ~79 |
| NMCO/Cu-foil NWAs | ~50 |
| NMCO/Cu-foam NWAs | ~40 |



* The Mg and Al in the EDS spectra due to the stainless steel sample stage used for SEM.

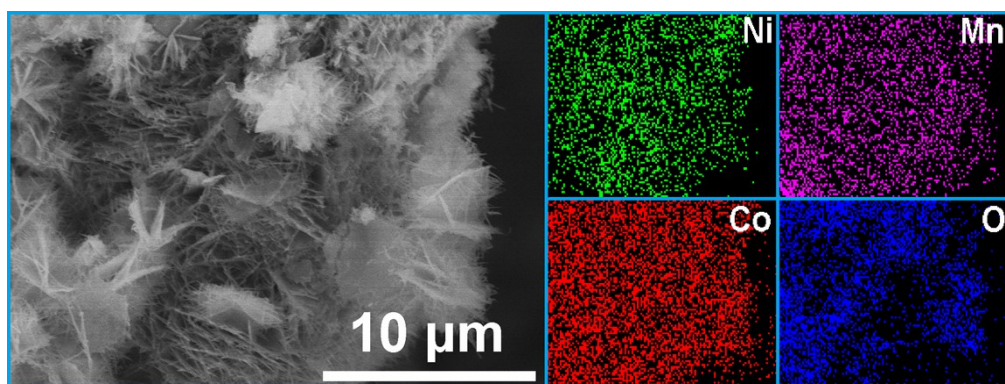


Fig.S5 The EDS patterns of NMCO/Cu-foam NWAs and its EDS elemental mappings.

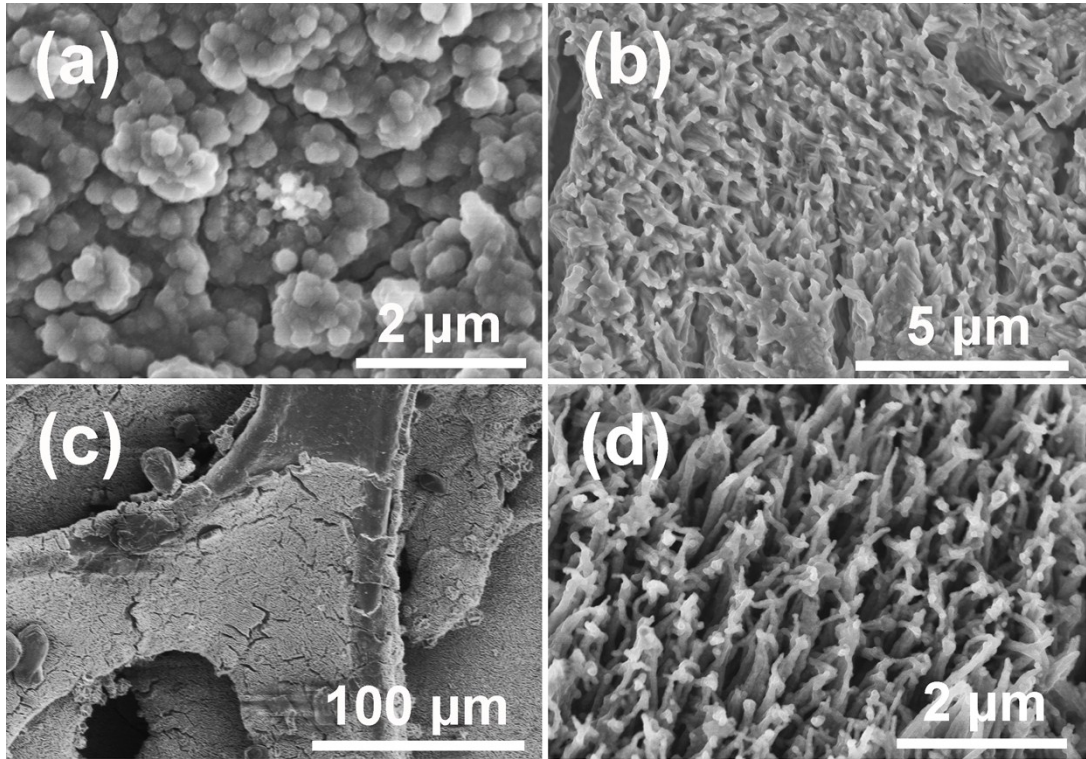


Fig.S6 High magnification SEM images of (a) NMCO NWs and (b) NMCO/Cu-foil NWAs, and (c) Low and (d) high magnification SEM images of NMCO/Cu-foam NWAs, all after 100 cycles at 0.2 A g^{-1} .

Tab.S3 Electrochemical performance of different TMOs electrodes.

| Type of materials | Initial charge capacity | Capacity retention rate |
|---|---|---|
| This work | 1501 mAh g^{-1} at 0.2 A g^{-1} | 98.2% (After 100 cycle at 0.2 A g^{-1}) 87.2% (After 100 cycle at 1 A g^{-1}) |
| NMCO multi-shell hollow microsphere ¹ | 1470 mAh g^{-1} at 0.2 A g^{-1} | 74.6% (After 250 cycle at 0.2 A g^{-1}) |
| NMCO inverse opal ² | 1003 mAh g^{-1} at 0.2 A g^{-1} | 23% (After 100 cycle at 0.15 A g^{-1}) |
| NMCO microspheres ³ | 1173 mAh g^{-1} at 25 mA g^{-1} | 37% (After 100 cycle at 25 mA g^{-1}) |
| $\text{Mn}_{0.54}\text{Ni}_{0.13}\text{Co}_{0.13}(\text{CO}_3)_{0.8}$ multi-shell-structured ⁴ | 806 mAh g^{-1} at 0.25 A g^{-1} | 56% (After 100 cycle at 0.25 A g^{-1}) |
| NiCo_2O_4 microspheres ⁵ | 1198 mAh g^{-1} at 0.25 A g^{-1} | 59% (After 500 cycle at 0.8 A g^{-1}) |
| $\text{NiCo}_2\text{O}_4@\text{C}$ fiber nanowire arrays ⁶ | 1357 mAh g^{-1} at 0.2 A g^{-1} | 84% (After 100 cycle at 0.5 A g^{-1}) |
| NiCo_2O_2 nanosheets@ CNT composites ⁷ | 1031 mAh g^{-1} at 0.2 A g^{-1} | a discharge capacity of 1309 mA h g^{-1} ¹ after 300 cycles at 0.4 A g^{-1} |
| CoNi_2O_2 nanosheets assembled flowers ⁸ | 617 mAh g^{-1} at 0.1 A g^{-1} | 66% (After 110 cycle at 0.1 A g^{-1}) |
| Co_3O_4 mesoporous nanoplates ⁹ | 2235 mAh g^{-1} at 44.5 mA g^{-1} | 50% (After 100 cycle at 44.5 mA g^{-1}) |
| $\text{Co}_3\text{O}_4/\text{Ni}$ foam | 1327 mAh g^{-1} at 0.2 A g^{-1} | 71% (After 100 cycle at 0.2 A g^{-1}) |

| | | |
|---|---|--|
| nanowires ¹⁰ | | |
| CNTs-entangled Mn ₃ O ₄ octahedrons ¹¹ | 780 mAh g ⁻¹ at 0.19 A g ⁻¹ | 83% (after 400 cycles at 468 A g ⁻¹) |
| Mn ₃ O ₄ @RGO nanowires ¹² | 802 mAh g ⁻¹ at 0.1 A g ⁻¹ | 87.5% (after 100 cycles at 0.1 A g ⁻¹) |

References

1. D. Luo, Y. P. Deng, X. Wang, G. Li, J. Wu, J. Fu, W. Lei, R. Liang, Y. Liu, Y. Ding, A. Yu and Z. Chen, *ACS Nano*, 2017, **11**, 11521-11530.
2. D. McNulty, H. Geaney and C. O'Dwyer, *Sci Rep*, 2017, **7**, 42263.
3. Z. Xie, J. Zhao and Y. Wang, *Electrochim. Acta*, 2015, **174**, 1023-1029.
4. J. Q. Zhao and Y. Wang, *J. Mater. Chem. A*, 2014, **2**.
5. J. Li, S. Xiong, Y. Liu, Z. Ju and Y. Qian, *ACS Appl. Mater. Interfaces*, 2013, **5**, 981-988.
6. L. Shen, Q. Che, H. Li and X. Zhang, *Adv. Funct. Mater.*, 2014, **24**, 2630-2637.
7. X. Xu, B. Dong, S. Ding, C. Xiao and D. Yu, *J. Mater. Chem. A*, 2014, **2**, 13069-13074.
8. Y. Liu, Y. Zhao, Y. Yu, M. Ahmad and H. Sun, *Electrochim. Acta*, 2014, **132**, 404-409.
9. D. Su, X. Xie, P. Munroe, S. Dou and G. Wang, *Sci Rep*, 2014, **4**, 6519.
10. J. Zheng and B. Zhang, *Ceram. Int.*, 2014, **40**, 11377-11380.
11. C. Xia, Y. Wang, Q. Xu, P. Sun, X. Wang, T. Wei and Y. Sun, *Nanotechnology*, 2017, **28**.
12. J. G. Wang, D. Jin, R. Zhou, X. Li, X. R. Liu, C. Shen, K. Xie, B. Li, F. Kang and B. Wei, *Acs Nano*, 2016, **10**, 6227-6234.